Microbes and Infection 26 (2024) 105249

Contents lists available at ScienceDirect

Microbes and Infection

journal homepage: www.elsevier.com/locate/micinf

Original article

A new *Salmonella enterica* serovar that was isolated from a wild sparrow presents a distinct genetic, metabolic and virulence profile

Emiliano Cohen [a], Shalevet Azriel [a], Oren Auster [a, b, c], Adiv Gal [d], Svetlana Mikhlin [e], Sam Crauwels [f], Galia Rahav [a, b], Ohad Gal-Mor [a, b, c, *]

[a] *The Infectious Diseases Research Laboratory, Sheba Medical Center, Tel-Hashomer, Israel*
[b] *Faculty of Medicine, Tel Aviv University, Tel Aviv, Israel*
[c] *Department of Clinical Microbiology and Immunology, Tel Aviv University, Tel Aviv, Israel*
[d] *Faculty of Sciences, Kibbutzim College, Tel-Aviv, Israel*
[e] *Biovac Ltd., Or-Akiva, Israel*
[f] *Laboratory for Process Microbial Ecology and Bioinspirational Management (PME&BIM), Centre of Microbial and Plant Genetics (CMPG), Department of Microbial and Molecular Systems (M2S), KU Leuven, Leuven, Belgium*

ARTICLE INFO

Article history:
Received 27 August 2023
Accepted 6 November 2023
Available online 11 November 2023

Keywords:
Salmonella
Virulence
Pathogenicity
Host-specificity
Salmonellosis
Inflammation

ABSTRACT

Salmonella enterica is a ubiquitous and clinically-important bacterial pathogen, able to infect and cause different diseases in a wide range of hosts. Here, we report the isolation and characterization of a new *S. enterica* serovar (13,23:i:-; *S.* Tirat-Zvi), belonging to the Havana supper-lineage that was isolated from a wild house sparrow (*Passer domesticus*) in Israel. Whole genome sequencing and complete assembly of its genome indicated a plasmid-free, 4.7 Mb genome that carries the *Salmonella* pathogenicity islands 1–6, 9, 19 and an integrative and conjugative element (ICE), encoding arsenic resistance genes. Phenotypically, *S.* Tirat-Zvi isolate TZ282 was motile, readily formed biofilm, more versatile in carbon source utilization than *S.* Typhimurium and highly tolerant to arsenic, but impaired in host cell invasion. In-vivo infection studies indicated that while *S.* Tirat-Zvi was able to infect and cause an acute inflammatory enterocolitis in young chicks, it was compromised in mice colonization and did not cause an inflammatory colitis in mice compared to *S.* Typhimurium. We suggest that these phenotypes reflect the distinctive ecological niche of this new serovar and its evolutionary adaptation to passerine birds, as a permissive host. Moreover, these results further illuminate the genetic, phenotypic and ecological diversity of *S. enterica* pathovars.

Salmonella enterica is a Gram-negative facultative intracellular bacterium that can infect a remarkable range of animal hosts [1] and even plants [2]. *Salmonella* infection in animals and humans can lead to various clinical outcomes ranging from asymptomatic colonization, self-limited gastroenteritis, bacteremia, to a disseminated systemic infection, known as enteric or typhoidal fever [3]. The ability of *Salmonella* to infect different hosts including food producing animals that serves as the main zoonotic reservoir for human infections, makes *Salmonella* a leading foodborne pathogen. Each year, non-typhoidal *Salmonella* (NTS) are responsible for 94 million gastroenteritis cases in humans and 155,000 deaths globally [4]. The single species *S. enterica* is a highly diverse pathogen consisting of more than 2600 antigenically distinct serovars that are defined according to the Kauffman–White–Le Minor classification scheme, according to the expression of somatic (lipopolysaccharide), flagellar and capsular determinants, known as O, H and Vi antigens, respectively [5].

This broad collection of known *S. enterica* serovars can be divided into three phenotypic groups according to their host-specificity profile [6]. Most of the non-typhoidal salmonellae such as *S. enterica* serovar Typhimurium (*S.* Typhimurium), *S. enterica* serovar Enteritidis (*S.* Enteritidis), or *S. enterica* serovar Infantis (*S.* Infantis) are host generalists, and can infect and colonize a wide range of hosts including poultry, livestock, wild rodents and humans [7]. In most cases (but not always), infection of adult animals by generalist *Salmonella* serovars results in an asymptomatic colonization, but transmission to immunocompetent humans will present as a self-limiting acute gastroenteritis. The second group is

* Corresponding author. The Infectious Diseases Research Laboratory, Sheba Medical Center, Tel-Hashomer 5262100, Israel.
E-mail address: Ohad.Gal-Mor@sheba.health.gov.il (O. Gal-Mor).

https://doi.org/10.1016/j.micinf.2023.105249
1286-4579/

host-specific serovars, which were evolved to infect and cause a typhoid-like disease in only one or a few host-species. For instance, *S*. Typhi, *S*. Paratyphi A and *S*. Sendai can infect only humans or higher primates, that will lead to a systemic, life-threatening enteric fever disease. Similarly, *S*. Gallinarum (and its biovar, Pullorum) are restricted to poultry and cause systemic invasive diseases known as fowl typhoid and pullorum disease, respectively [8]. A third group consists host-adapted serovars that frequently cause a severe systemic disease in one main host, but occasionally a spillover to other hosts, including humans occurs. Examples include *S*. Choleraesuis (swine adapted), *S*. Dublin (bovine adapted) and *S*. Abortusovis (goats and sheep adapted) [9].

Multiple virulence factors have been demonstrated to shape *Salmonella* pathogenesis including its signature virulence-associated capabilities to invade non-phagocytic host cells and replicate within professional phagocytes. *Salmonella* pathogenicity requires a synchronized function of both *Salmonella*-conserved and serovar-specific virulence factors that include fimbrial adhesins, invasion factors (e.g., SiiE, MisL, ShdA) and genes expressed from *Salmonella* Pathogenicity Island (SPI) − 1 and 2 (reviewed in Refs. [10,11]) and other SPIs [12]. SPIs 1 and 2 encode two different type III secretion systems (T3SSs) and designated translocated effectors involved in modifying multiple host programs during certain stages of the infection [12]. While SPI-1-encodes the T3SS-1 that plays an important role in intestinal invasion and subversion of the host-immune response, the second type III secretion apparatus, encoded on SPI-2 (T3SS-2) is needed for intracellular survival and replication of *Salmonella* within phagocytic cells [13].

Previous studies demonstrated that certain pathovars of *S*. Typhimurium have evolved to become adapted to wild birds [14]. For instance, *S*. Typhimurium definitive phage type (DT) 2 and DT99 are host-adapted and produce a fatal systemic disease in *Columba livia* (rock or feral pigeon) [15], while DT40 and DT56 are associated with salmonellosis in passerine birds [16,17]. Recently, we reported a genetic, phenotypic and virulence characterization of a monophasic *S*. Typhimurium strain that was isolated from several wild sparrows in Israel and demonstrated unique phenotypic and genetic signatures that are likely to contribute to its pathoadaptation to passerine birds [18]. Here, we describe the isolation, whole genome sequencing (WGS), phenotypic characterization and virulence profiling of a previously uncharacterized *S. enterica* serovar (*S*.13,23:i:-) that was isolated from a wild house sparrow (*Passer domesticus*) and demonstrate its different pathogenicity in young chicks and the mouse models.

1. Materials and methods

1.1. Salmonella *isolation and bacterial strains*

Bacterial strains used in this study are listed in Table S1. *Salmonella* isolation from wild birds was previously described [18] and more details are given in the Supplementary Material section.

1.2. *Whole genome sequencing and bioinformatics*

Culture of *S*. Tirat-Zvi isolate TZ282 that was grown in LB was used to extract DNA using the GenElute Bacterial Genomic DNA Kit (Sigma–Aldrich). Whole genome sequencing that was performed at the Technion Genomic Center (Haifa, Israel) has generated 299,256 long reads (mean: 9875 bp; N50: 28,276 bp) using a MinION sequencer (Oxford Nanopore Technologies) and 2.9 × 10^6 paired-ends 250 bp reads by an Illumina MiSeq platform (Illumina, Inc.). Trycycler was used to *de novo* assemble of the genome from the long reads, which was then polished with the short reads to correct possible sequencing errors. The assembled complete genome resulted in sequencing depth of 615×. The 4,772,725 bp complete, gap-free genome of *S*. Tirat-Zvi TZ282 was deposited at NCBI under accession number CP122457 (BioProject number PRJNA954863). The NCBI Prokaryotic Genome Annotation Pipeline (PGAP) v6.5 [19] was used to annotate *S*. Tirat-Zvi genome, using the default parameters.

Hierarchical Clustering (HierCC) analysis in EnteroBase based on a core-genome MLST [20], was used to identify the super-lineage (HC2000) of *S*. Tirat-Zvi. The identified HC2000_6515 contained 64 strains and a NINJA neighbor-joining (NJ) GrapeTree [21] was built in Enterobase to describe the population structure of HC2000_6516 in relation to additional selected strains from subspecies I, II, IIIa, and IIIb. All the genome assemblies used to build this tree are listed in Table S3.

1.3. *Gene deletion and cloning*

Primers used in this study are listed in Table S2. *S*. Tirat-Zvi *clpV* null mutant strain was constructed by the λ-red-recombination system [22], using the primers P1_ClpV and P2_ClpV. A 1600-bp amplimer containing the kanamycin resistance cassette was integrated into the genome of *S*. Tirat-Zvi TZ282 and replaced the *clpV* locus. The resistance gene was latter excised by the pCP20 helper plasmid encoding the FLP recombinase. The resulted *clpV* null deletion was verified by Sanger sequencing using the primers Clpv_flank_5_Fwd and ClpV_flank_3_Rev (Table S2).

To complement the expression of *clpV* in *S*. Tirat-Zvi, this gene was PCR-amplified using the primers Gibson_clpV_fwd and Gibson_clpV_rev. The obtained PCR fragment was digested with KpnI and HindIII and cloned using the Gibson assembly [23] into pWSK29.

1.4. *Reverse transcription real-time PCR*

qRT-PCR was conducted as described in Ref. [24]. More details are given in the Supplementary Material section.

1.5. *Motility assay*

The motility phenotype was studied on soft (0.3%) agar plates at 37 °C as we previously described [25].

1.6. *Phenotypic microarrays*

The Biolog Phenotypic MicroArray analysis was conducted following the manufacturers recent protocol for *Escherichia coli* and other Gram-negative bacteria using redox dye. Briefly, *Salmonella* strains were precultured on LB agar plates, which were incubated at 37 °C for 48 h. Colonies from the agar plates were picked with a cotton swab and transferred to the Biolog inoculation fluid (IF-0 GN/GP) until a transmittance of 85% was reached. After the addition of redox dye A (1:100), 100 μl of the solution was added to each well and the Biolog Phenotypic Microarray plates (carbon plates PM1 and 2) were incubated in the OmniLog PM system for 48 h maintaining a temperature of 37 °C under aerobic conditions.

1.7. *Biofilm formation*

Biofilm formation was evaluated as we previously described [25] and more details are given in the Supplementary Material section.

1.8. Arsenic resistance

Serial dilutions of *Salmonella* cultures that were grown for 16 h in LB medium at 37 °C, were spotted onto LB agar plates supplemented with 0.05, 0.1, 0.5 and 1 mM arsenate (Na_3AsO_4) or arsenite ($NaAsO_2$). The plates were incubated for overnight at 37 °C and imaged directly using Fusion SOLO X system (VILBER).

1.9. Host cell invasion and replication tissue cultures

Host cell infection assay was conducted using the gentamicin protection assay as in Ref. [18]. For more details, please see the Supplementary Material section.

1.10. Chick infection model

One-day-old SPF white Leghorns chicks (Charles River) were infected with *Salmonella* strains according to the ethical requirements of the Animal Care Committee of the Sheba Medical Center (Approval number 1059/16) and in line with the guidelines of the National Council for Animal Experimentation as we recently reported [18]. The chicks were infected orally (intra crop) with 5–8 $\times$ 10^6 CFU of ampicillin-resistant *Salmonella* strains that were grown for overnight in LB medium. Three- to four-days post infection (p.i), the intestines and systemic organs were aseptically collected on ice and homogenized in saline (0.9% NaCl). Serial dilutions were plated on XLD agar plates supplemented with ampicillin to determine the bacterial load in each tissue sample.

1.11. Mouse infection model

Experiments in the mouse model were conducted according to the ethical requirements of the Animal Care Committee of the Sheba Medical Center (Approval # 1182/18) and in line with the national guidelines. 24 h before the infection, seven week-old Female C57/BL6 mice (Envigo, Israel) were pretreated with streptomycin (20 mg per mouse) by gavage needle. *S*. Tirat-Zvi and *S*. Typhimurium strains harboring pWSK29 (ampicillin-resistance low copy-number plasmid) were grown in LB medium supplemented with ampicillin for overnight at 37 °C and diluted in 0.2 ml saline. Mice were orally infected using oral gavage with ~1 $\times$ 10^6 CFU of each strain. Four-days p.i, mice were euthanized and tissues were aseptically harvested on ice. Serial dilutions of the tissue homogenates were plated on XLD agar under ampicillin selection, incubated at 37 °C and counted to calculate bacterial loads.

1.12. Histology

Cecal samples were fixed in 10% neutral buffered formalin for 24 h and then embedded in paraffin. 5 μm sections were stained with Hematoxylin and Eosin (H&E). Pictures were taken using Olympus BX60 Microscope at objective magnification of $\times$10 and imaged with Olympus DP73 digital camera.

1.13. Cytokine expression in vivo

Cecal samples obtained from mice were immersed in RNAlater Stabilization Reagent (QIAGEN). Total RNA was extracted using RNeasy Plus Mini Kit (QIAGEN) and reverse transcribed into cDNA, using the qScript cDNA synthesis kit (Quantabio). qRT-PCR was done using Fast SYBR Green Master Mix (Applied Biosystems) and cytokines-specific primers (Table S2) on a StepOnePlus Real-Time PCR System. Data were normalized to the house-keeping gene *Gapdh* and fold change was calculated as $2^{-\Delta\Delta Ct}$.

2. Results

2.1. Isolation of a new S. enterica serovar from a wild sparrow and its genomic characterization

During a microbial ecology pilot survey, aiming to estimate the prevalence of *Salmonella* spp. in wild birds in Israel, we have sampled more than 400 wild birds at different geographical sites across Israel. Using non-invasive cloacal swabs and culturing in a Rappaport-Vassiliadis selective enrichment broth, we were able to isolate five *S. enterica* isolates from three House Sparrows (*P. domesticus*) and two Spanish Sparrows (*Passer hispaniolensis*). As we recently reported [18], four isolates were passerine-adapted monophasic *S*. Typhimurium that were isolated in a single site at the coastal plain to the north of Tel-Aviv, and the fifth isolate (designated TZ282) was obtained from a female House Sparrow in the Jordan Valley near Kibbutz Tirat-Zvi (32.417723 N 35.53676 E). Interestingly, serotyping of isolate TZ282 at the national *Salmonella* reference center, according to the Kauffman–White–Le Minor scheme, indicated a group G monophasic serovar with a previously-undocumented antigenic formula of 13,23:i:-.

Strain search in Enterobase [26], for additional *Salmonella* records with the same antigenic formula (13,23:i:-) did not identify another strain from this serovar. Similarly, whole genome sequencing of isolate TZ282 genome and a phylogenetic analysis, indicated no representation of the same sequence type (ST_209950) or clonal complex (HC900_209950) among the 415,559 *Salmonella* genomes deposited in Enterobase (as for Aug. 2023). Therefore, we concluded that this is a previously uncharacterized serovar and named it *S. enterica* serovar Tirat-Zvi (*S*. Tirat-Zvi). Hierarchical Clustering (HierCC) analysis in EnteroBase using a core-genome MLST, based on 3002 genes [27] indicated that *S*. Tirat-Zvi belonging to a specific *S. enterica* subsp. I super-lineage (HC2000) designated 6515. This lineage contains 64 strains that together consists five HC900 clusters, the equivalent of eBURST groups [20], which also correlates strongly with the serovar classification [26,28]. Three of these clusters (HC900_6515, 114237, and 85039) correspond to serovar Havana, one cluster (HC900_191912) to serovar Romanby and another cluster (HC900_209950) is the newly defined *S*. Tirat-Zvi. Fig. 1A shows a NINJA neighbor-joining (NJ) GrapeTree that illustrates the population structure of HC2000_6515 and the phylogenetic relationship of *S*. Tirat-Zvi to other *Salmonella* serovars within and outside of this lineage (Table S3).

To generate a gap-free complete assembly of *S*. Tirat-Zvi TZ282, we have implemented hybrid genome assembly, using both short (Illumina) and long (Oxford Nanopore) sequencing reads. The assembled plasmid-free genome of *S*. Tirat-Zvi TZ282 (Accession number CP122457) is 4,772,725 bp long, and has a G + C content of 52.3%. Using the NCBI Prokaryotic Genome Annotation Pipeline (PGAP) we predicted that *S*. Tirat-Zvi TZ282 genome encodes 4575 genes, 4455 CDSs, 84 tRNA genes and 123 pseudogenes (Table S4). Sequence analysis indicated that *S*. Tirat-Zvi harbors intact SPIs 1 to 5 and SPI-9 (Fig. 1B), however, in addition to these conserved SPIs, *S*. Tirat-Zvi TZ282 also carries SPI-6 (Fig. S1) and SPI-19 (Fig. S2), both encode a type VI secretion system (T6SS) that was previously linked to colonization of the host-adapted *Salmonella* serovars Dublin, Gallinarum, and Pullorum [29–31]. Whole genome sequencing also indicated the absence of the flagellar phase variation DNA invertase *hin* (WP_000190912) that is consistent with the monophasic nature of its flagellar antigens.

Moreover, *S*. Tirat-Zvi TZ282 was found to harbor an extensive fimbriome with at least 14 chaperon-usher fimbria gene clusters including Sta, Lpf, Std, Ste, Yeh, Fim, Stb, Tcf, Saf, Stf, Sti, Bcf, Sth, and

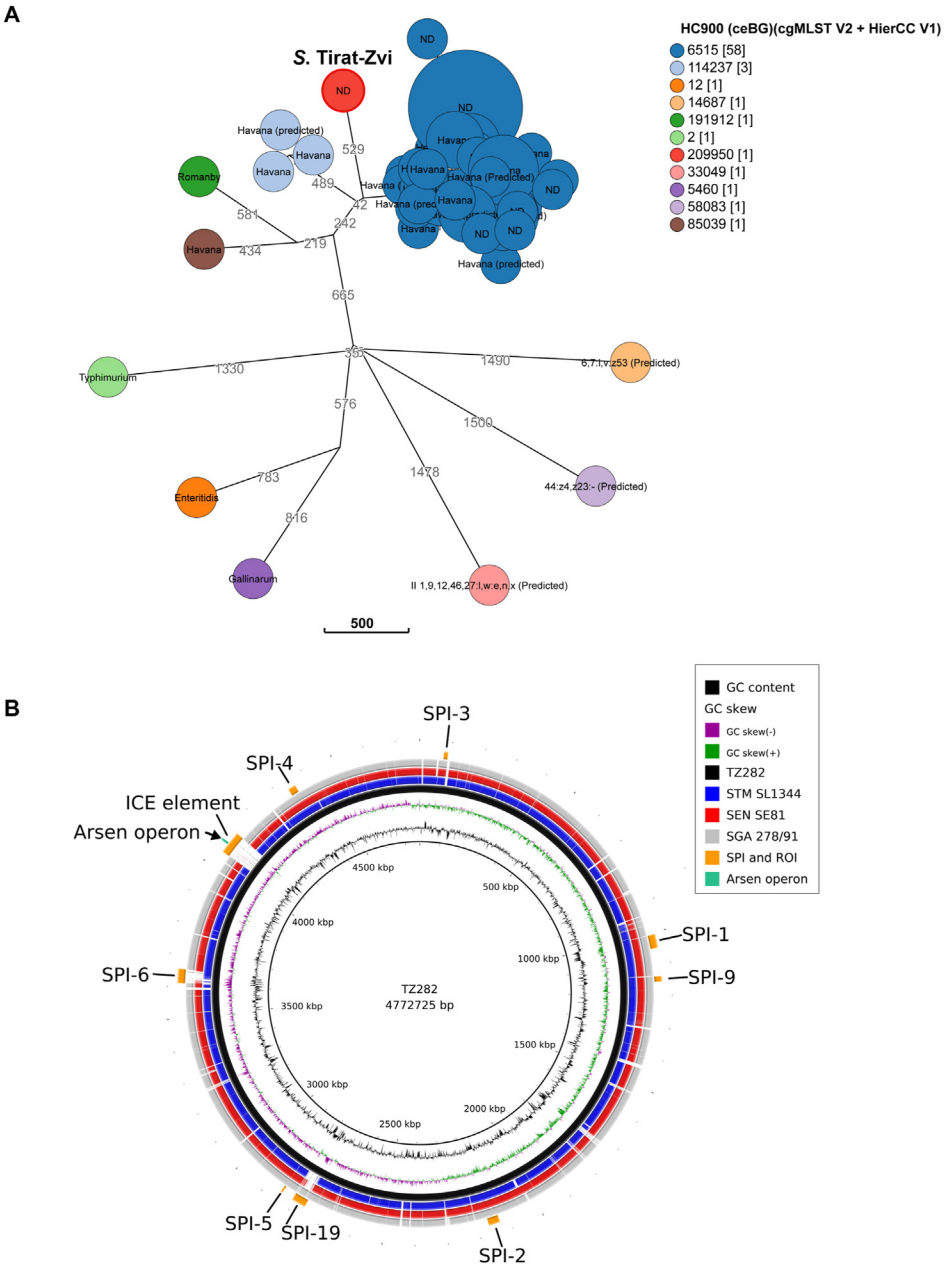

Fig. 1. Whole genome sequencing and phylogenetic analysis of the new *S.* Tirat-Zvi serovar. (**A**) A NINJA neighbor-joining (NJ) GrapeTree of *S.* Tirat-Zvi (highlighted in red) and the complete genomes of additional 71 strains was constructed in Enterobase using the core-genome MLST scheme (3002 genes). The tree nodes are color-coded by HC900 data, the equivalent of eBURST groups and the size of the nodes reflects the number of strains within each node. The mane of the serovar is indicated inside the nodes and the branch length varies according to the distance between nodes, while indicating the number of cgMLST allelic differences, which is also shown by the scale bar. The tree encompasses all 64 HC2000_6515 genomes composing this super-lineage, recorded in EnteroBase (as for 10 August, 2023 at which time-point EnteroBase contained >415,000 *Salmonella* genomes) and additional selected isolates of interest to put HC2000_6515 in a broader phylogenetic context, including strains from other subspecies I lineages (Typhimurium and Enteritidis), subspecies II (1,9,12,46,27:l,w:e,n,x), subspecies IIIa (44:z4,z23:-), and subspecies IIIb (6,7:l,v:z53). All the strains that were used to construct this tree and their metadata are listed in Table S3. **(B)** The genome sequence of *S.* Tirat-Zvi isolate TZ282 in comparison to the genomes of *S.* Typhimurium SL1344 (accession number NC_016810.1), *S.* Enteritidis SE81 (accession number NZ_CP050721.1), and *S.* Gallinarum 278/91 (accession number AM933173.1) was created by BLAST Ring Image Generator (BRIG). The presence and location of the different *Salmonella* pathogenicity islands and the ICE-encoding the *ars* operon are shown by orange boxes. The chromosome sequence of this isolate was deposited at NCBI under accession number CP122457 (BioProject number PRJNA954863).

Stj, in addition to the non-fimbrial adhesion SiiE and the Csg curli fimbria (Fig. S3). Interestingly, the *sta, fim, tcf* and *saf* fimbrial clusters were adjacent to transposase or integrase genes, and in the case of *sta* and *fim* also in proximity to a tRNA gene, suggesting that these clusters were acquired via horizontal gene transfer into the *S.* Tirat-Zvi core genome [32].

2.2. *S. Tirat-Zvi can utilize diverse carbon sources better than S. Typhimurium*

To better understand the ecology and biology of *S.* Tirat-Zvi, we chose to compare various phenotypes with the well-characterized broad-host serovar *S.* Typhimurium as a reference. Comparison of

metabolic reconstruction between *S.* Tirat-Zvi and *S.* Typhimurium, using the RAST tool [33], has indicated the presence of several carbohydrates pathways that are functional in *S.* Tirat-Zvi, but not in *S.* Typhimurium including maltose, maltodextrin, lactose and galactose uptake and utilization (Table S5). To identify possible metabolic differences between *S.* Tirat-Zvi and *S.* Typhimurium, we have used the Biolog Phenotype MicroArrays (PMs) platform that allowed us to compare the metabolism (substrates oxidization) of these serovars in the presence of 190 different carbon sources. This analysis indicated that while *S.* Tirat-Zvi and *S.* Typhimurium can metabolize D-glucose-1-Phosphate (Fig. 2A) as a carbon source at similar levels at the stationary phase, *S.* Tirat-Zvi can oxidize better than *S.* Typhimurium multiple carbohydrates including lactose (Fig. 2B) maltose (Fig. 2C), galactose (Fig. 2D) and mannitol (Fig. 2E). In contrast, *S.* Tirat-Zvi did not metabolize the hexose monosaccharide tagatose, while *S.* Typhimurium did (Fig. 2F). Growth curves in M9 minimal medium, which was supplemented with glucose (Fig. 2G) or maltose (Fig. 2H), as the single carbon source, confirmed the corresponding PMs results and demonstrated similar and superior growth, respectively of *S.* Tirat-Zvi in comparison to *S.* Typhimurium. Moreover, *S.* Tirat-Zvi was found to metabolize much better than *S.* Typhimurium different organic acids including glyoxylic acid, tricarballylic acid, α-keto-glutaric acid, D-arabinose and 2-deoxy-D-ribose (Data not shown), suggesting that *S.* Tirat-Zvi is more versatile and efficient in carbon source utilization than *S.* Typhimurium.

2.3. *S. Tirat-Zvi is motile, readily forms biofilm and is highly tolerant to arsenic*

Considering the genetic profile of *S.* Tirat-Zvi [e.g. the mutation in *hin* and its fimbriome encoded genes (Fig. S3)] and its possible association with an avian host, we were interested in characterizing environmentally-relevant phenotypes of this serovar. Specifically, we were interested in studying the motility and biofilm formation of *S.* Tirat-Zvi, as previous reports have shown that the poultry-associated serovars, *S.* Gallinarum and *S.* Pullorum are not motile and weak biofilm producers [34,35]. Additionally, we sought out to test the resistance of *S.* Tirat-Zvi to arsenic compounds, due to the uncommon presence of the of the *ars* cluster (see below). Motility assay on soft agar plates together with *S.* Typhimurium SL1344 that was included as a positive control and the non-motile *S.* Gallinarum 287/91 as a negative control [36] showed a comparable motility of *S.* Tirat-Zvi TZ282 to the one of *S.* Typhimurium SL1344 (Fig. 3A). Moreover, *S.* Tirat-Zvi TZ282 readily formed biofilm, at levels that were higher than those of *S.* Typhimurium SL1344. The negative control *S.* Gallinarum that lacks flagellum, were unable to form biofilm under these experimental conditions (Fig. 3B). These results indicated that the lack of the second phase flagellar antigen expression does not impair the motility nor biofilm formation of this serovar.

Interestingly, we found that *S.* Tirat-Zvi TZ282 genome harbors a 68 kb integrative and conjugative element (ICE) that carries an

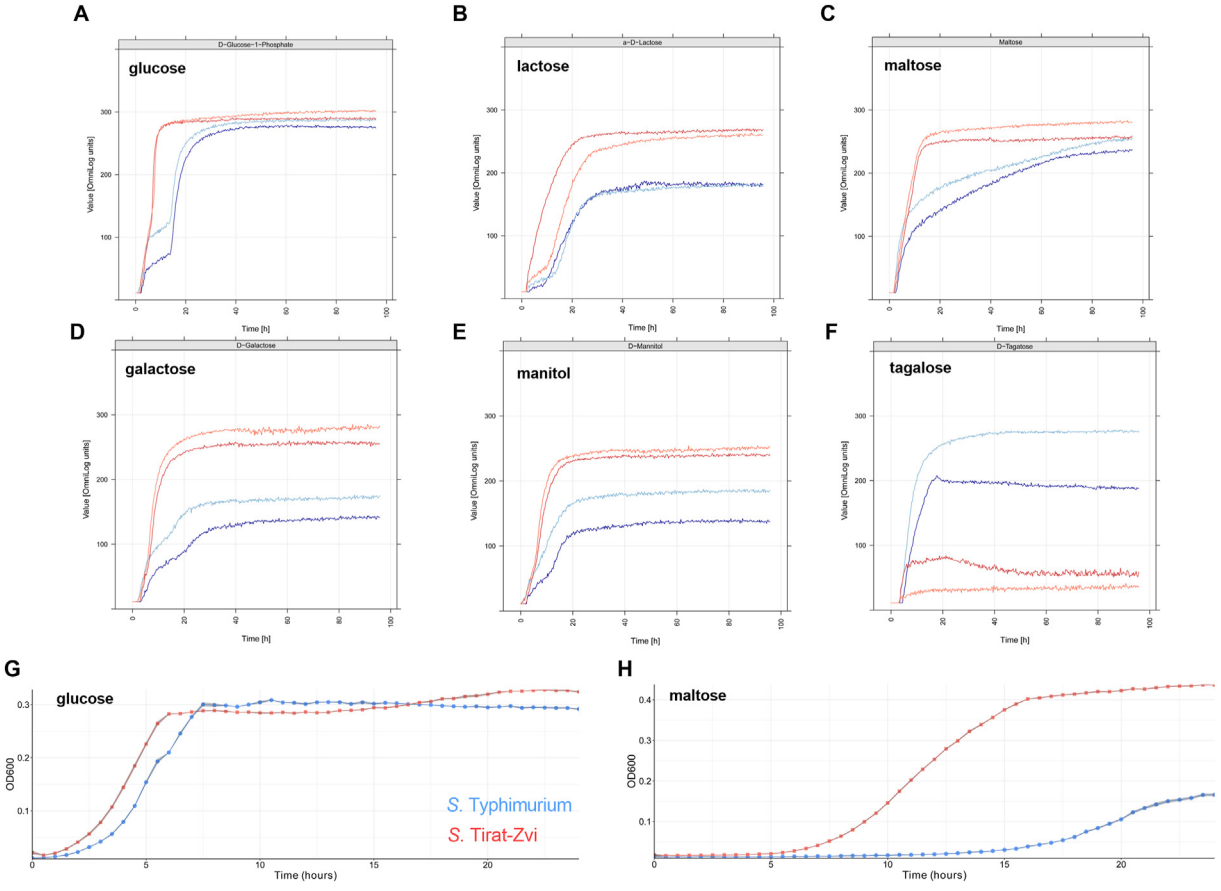

Fig. 2. Differences in carbon source utilization between *S.* Tirat-Zvi and *S.* Typhimurium. The Biolog Phenotypic MicroArray (PM1 and PM2) were used to determine the oxidation of 190 carbon sources by *S.* Tirat-Zvi TZ282 and *S.* Typhimurium SL1344 at 37 °C under aerobic growth conditions. The reduction of the tetrazolium reporter dye to a visible purple color was used as an indicator of microbial metabolism and was measured by the Biolog OmniLog® instrument. Carbon source utilization is shown as the reading of OmniLog units over time. The results of carbon source utilization for glucose (**A**), lactose (**B**), maltose (**C**), galactose (**D**), mannitol (**E**) and tagalose (**F**) is presented for two independent experiments for *S.* Tirat-Zvi (in shades of red) and *S.* Typhimurium (in shades of blue). Standard growth curves of *S.* Typhimurium SL1344 and *S.* Tirat-Zvi cultures that were grown at 37 °C in minimal M9 medium supplemented with 11 mM glucose (**G**) or maltose (**H**) as the sole carbon source is presented.

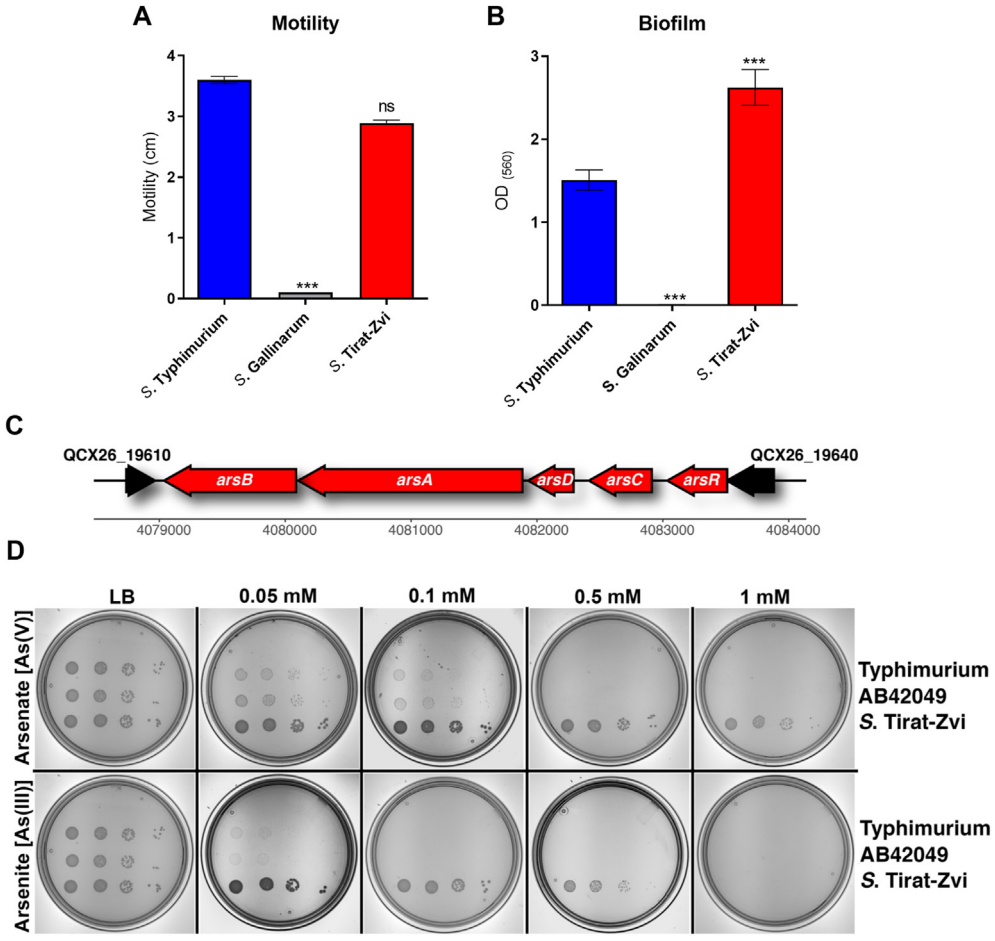

Fig. 3. *S.* Tirat-Zvi is motile, forms high levels of biofilms and is arsenic tolerant. (**A**) The motility of *S.* Typhimurium strain SL1344, *S.* Tirat-Zvi TZ282 and *S.* Gallinarum strain 287/91 (that was included as a negative control) was evaluated by swimming on soft (0.3%) agar LB plates at 37 °C. The swimming radius (in cm) after 5 h incubation is presented. The bars show the mean and the standard error of the mean (SEM) of 3–4 independent cultures. One-way ANOVA with Dunnett's Multiple Comparison Test was used to determine statistical difference in relation to *S.* Typhimurium. ns, not significant; ***, $P < 0.001$. (**B**) Biofilm formation by the above strains was determined by Crystal Violet staining of static cultures that were incubated for 96 h at 28 °C in rich LB broth in the absence of sodium chloride (biofilm induced conditions). Biofilm was quantified by the absorbance of the stained adherent cells at OD_{560}. The bars show the mean of six biological repeats and the SEM is indicated by the error bars. (**C**) The genetic organization of the arsenic tolerance (*ars*) operon in *S.* Tirat-Zvi TZ282 genome is shown. The corresponding chromosomal coordinates of *S.* Tirat-Zvi (accession number CP122457) are indicated at the bottom axis. (**D**) *S.* Typhimurium strain SL1344, the sparrow-associated strain AB42049 and *S.* Tirat-Zvi TZ282 were grown for overnight in LB medium to the stationary phase. Aliquots of serial dilutions were spotted onto LB-agar plates supplemented with increasing concentrations of arsenate (Na_3AsO_4) and arsenite ($NaAsO_2$) and imaged following incubation of 16 h at 37 °C.

arsenic resistance gene cluster encoded by the *arsABCDR* operon, which confers arsenic tolerance (Fig. 3C). In this system, ArsB functions as an arsenite efflux transporter; ArsA is an arsenical pump-driving ATPase; ArsC is an arsenate reductase; ArsD is an arsenite efflux transporter metallochaperone; and ArsR is a trans-acting helix-turn-helix transcriptional regulator. To phenotypically test arsenic tolerance by *S.* Tirat-Zvi TZ282, serial dilutions of stationary phase cultures were plated on LB agar plates supplemented with increasing concentrations of arsenate (Na_3AsO_4) and arsenite ($NaAsO_2$). As negative controls, cultures of *S.* Typhimurium SL1344 and the recently characterized sparrow adapted strain AB42049 [18] were also included in the assay. As presented in Fig. 3D, *S.* Tirat-Zvi TZ282, but not the *S.* Typhimurium strains was able to grow in the presence of 1 mM arsenate and 0.5 mM arsenite, suggesting that the *ars* operon is expressed and functional under standard laboratory growth conditions.

2.4. *S. Tirat-Zvi presents impaired invasion into non-phagocytic host cells*

To characterize virulence-associated phenotypes of *S.* Tirat-Zvi, we next studied the ability of this strain to invade and replicate within non-phagocytic host cells and to survive in macrophages, in comparison to *S.* Typhimurium. Interestingly, the invasion of *S.* Tirat-Zvi TZ282 into both human HeLa epithelial cells (Fig. 4A) and DF-1 chicken fibroblasts (Fig. 4C), but not uptake by U937 human macrophages (Fig. 4E) was significantly lower than *S.* Typhimurium SL1344. Additionally, we found that the intracellular replication of *S.* Tirat-Zvi is significantly reduced in DF-1 chicken fibroblasts (Fig. 4D), but not in HeLa (Fig. 4B) or U937 macrophages (Fig. 4F), in which *S.* Tirat-Zvi actually replicated even better compared to *S.* Typhimurium. We concluded from these experiments that while *S.* Tirat-Zvi is able to replicate at a similar or higher extent than *S.*

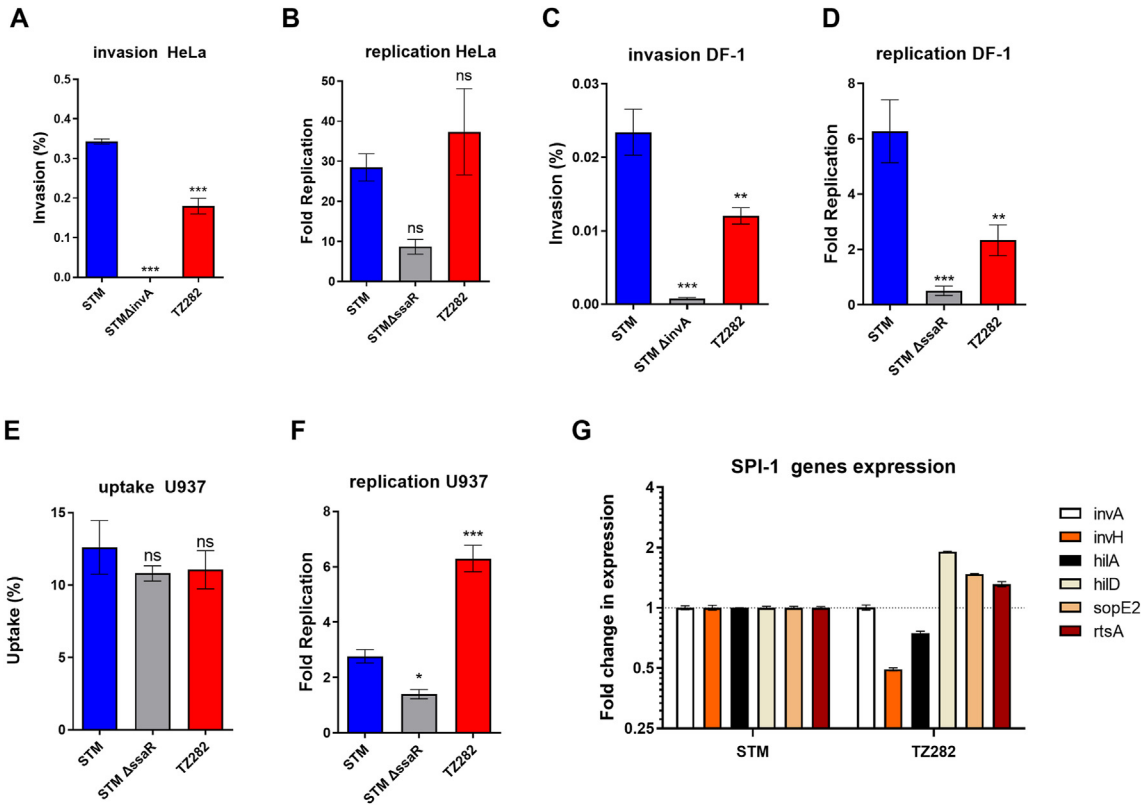

Fig. 4. *S.* Tirat-Zvi is impaired in host cell invasion. The invasion of *S.* Typhimurium SL1344 (STM), its isogenic T3SS-1 *invA* mutant strain (included as a negative control for invasion) and *S.* Tirat-Zvi TZ282 was tested by the gentamicin protection assay with HeLa human epithelial cells (**A**) and with DF-1 chicken fibroblasts (**C**). Invasion is presented as the percentage of intracellular bacteria at 2 h post infection (p.i.), from the infecting inoculum. Intracellular replication of *S.* Typhimurium SL1344, its isogenic T3SS-2 *ssaR* mutant strain (included as a negative control for intracellular replication), and *S.* Tirat-Zvi TZ282 was tested by the gentamicin protection assay with HeLa human epithelial cells (**B**) and with DF-1 chicken fibroblasts (**D**). Intracellular replication is presented as fold replication that was calculated by the ratio between the number of intracellular bacteria at 24 h p.i. relative to their intracellular load at 2 h p.i. Macrophage uptake (**E**) and intracellular replication (**F**) in human U937 macrophages was determined as above. The bars show the mean of 3–4 biological repeats and the SEM is indicated by the error bars. One-way ANOVA with Dunnett's Multiple Comparison Test was used to determine statistical difference from *S.* Typhimurium. ns, not significant; *, $P < 0.05$; **, $P < 0.01$; ***, $P < 0.001$. (**G**) RNA was extracted from *S.* Typhimurium SL1344 (STM) and *S.* Tirat-Zvi (TZ282) cultures that were grown to the late logarithmic phase in LB at 37 °C and was reverse transcribed. qRT-PCR was used to determine the fold change in expression of the SPI-1 genes *invA, ssaR, invH*, *hilA, hilD*, *sopE2* and *rtsA* in *S.* Tirat-Zvi vs. *S.* Typhimurium. The housekeeping genes *rpoD* and 16S rRNA were used for normalization of target genes. The indicated values show the mean of three biological repeats and the SEM is represented by the error bars.

Typhimurium in human host cells, its invasion into non-phagocytic human and avian cells is moderately impaired compared to *S.* Typhimurium.

To account if the impaired host cell invasion is due to lower expression levels of SPI-1 genes in *S.* Tirat-Zvi, as we previously showed for *S.* Infantis [37], we compared the transcription of four SPI-1 genes (*invA, invH, hilA*, and *hilD*), SPI-1 translocated effector gene, *sopE2* and the SPI-1 regulator gene *rtsA*, in *S.* Tirat-Zvi TZ282 and *S.* Typhimurium SL1344. With the exception of *invH* that presented about 2-fold lower transcription in *S.* Tirat-Zvi relative to *S.* Typhimurium, other SPI-1 genes exhibited comparable or even elevated (in the case of *hilD*) expression levels in *S.* Tirat-Zvi (Fig. 4G). These results suggested that the inferior invasion of *S.* Tirat-Zvi TZ282 into non-phagocytic cells is not the result of lower SPI-1 gene expression in this serovar.

2.5. *S. Tirat-Zvi causes severe enterocolitis in young chicks*

To characterize the pathogenicity potential of *S.* Tirat-Zvi, and determine its ability to infect and cause a disease in different hosts, one-day-old SPF White Leghorns chicks (Charles River) were infected with 5–8 $\times$ 10^6 CFU of *S.* Tirat-Zvi TZ282 or *S.* Typhimurium SL1344. At day-three post infection, the chicks were euthanized and systemic and intestinal organs were aseptically collected. Birds autopsy indicated inflamed jejunum and ileum in birds infected with *S.* Tirat-Zvi or *S.* Typhimurium and notably inflated cecum, in the chicks that were infected with *S.* Tirat-Zvi, but not in uninfected chicks or in the chicks that were infected with *S.* Typhimurium (Fig. 5A–C). Pathological analysis of cecal sections that were stained for Hematoxylin and Eosin (H&E) presented necrotic enteritis in chicks that were infected with either *S.* Typhimurium or *S.* Tirat-Zvi. Chicks infected with *S.* Typhimurium demonstrated diffuse necrosis of the lamina propria and the epithelial layers, cecal epithelium hyperplasia, and edema in the intestinal submucosa. Chicks infected with *S.* Tirat-Zvi presented necrotizing colitis with diffuse necrosis of the entire mucosa and loss of crypts architecture. Acute inflammation was demonstrated in all infected chicks by massive infiltration of heterophils, lymphocytes and macrophages (Fig. 5D–F).

Tissue homogenates that were plated on selective plates for bacterial load counting indicated similar levels of *Salmonella* colonization at the intestines and systemic sites of the *Salmonella*-infected chicks, with slightly higher bacterial burden in the liver of chicks that were infected with *S.* Typhimurium than with *S.* Tirat-Zvi (Fig. 5G and H). Collectively, these results demonstrated that *S.* Tirat-Zvi TZ282 can infect young birds, causes acute necrotic enteritis and colonizes the intestine and systemic sites at similar levels as *S.* Typhimurium SL1344.

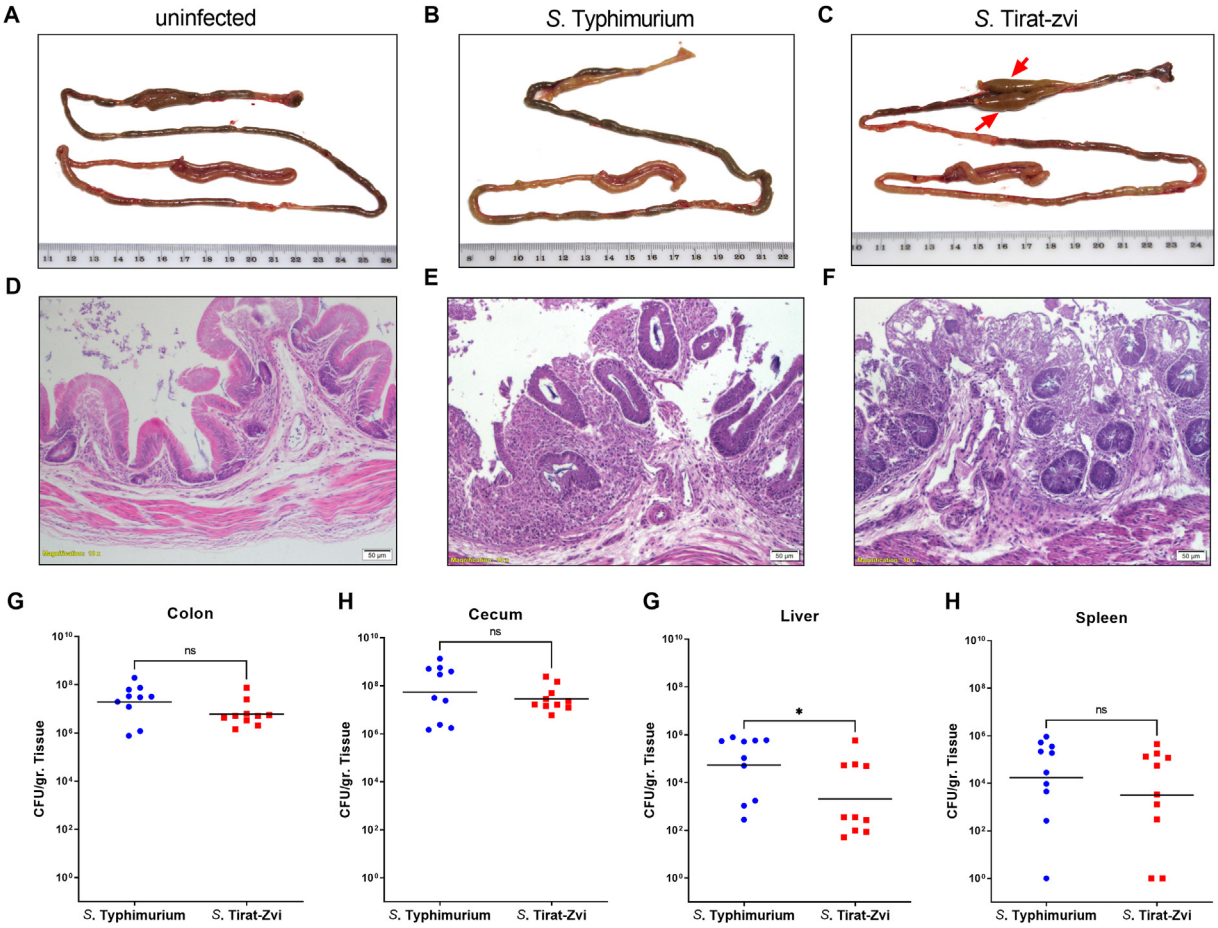

Fig. 5. *S.* Tirat-Zvi causes an acute inflammatory enterocolitis in the chick model. One-day old SPF chicks were directly inoculated intracrop with 5–8 × 10^6 CFU of *S.* Typhimurium SL1344 or *S.* Tirat-Zvi TZ282 carrying ampicillin resistance. Three days p.i., the birds were euthanized and the digestive tract of uninfected and infected chicks was imaged to assess the gross pathology of the gastrointestinal tract (**A**–**C**). Red arrowheads indicate the inflated cecum observed in chicks infected with *S.* Tirat-Zvi (**C**). × 100 magnification of H&E staining of cecal sections from an uninfected control (**D**) and chicks infected with *S.* Typhimurium (**E**) or *S.* Tirat-Zvi (**F**). Bar = 50 μm. Intestinal (cecum and colon) and systemic (liver and spleen) organs were aseptically isolated, weighted and homogenized in saline. Serial dilutions were plated on selective XLD plates for bacterial numeration in the colon (**G**), cecum (**H**), liver (**G**) and spleen (**H**). The experiment was conducted twice and combined data from two independent experiments are shown. Each dot represents data from one bird and horizontal lines show the geometrical mean of bacterial load per gram of tissue. A t-test was used to determine statistical significance (ns, not significant; *, $P < 0.05$).

2.6. S. Tirat-Zvi does not cause severe colitis the mouse host

To better define the host-specificity of *S.* Tirat-Zvi, we next examined the ability of this serovar to infect a mammalian host. C57BL/6 mice that were pretreated with streptomycin were infected with ~1 × 10^6 CFU of *S.* Typhimurium SL1344 or *S.* Tirat-Zvi TZ282 by oral gavage. In contrast to the similar level of colonization that was demonstrated by these serovars in the chick model, in the mouse, at four days post-infection, *S.* Tirat-Zvi colonization was several logs lower than *S.* Typhimurium in the cecum (Fig. 6A), ileum (Fig. 6B), colon (Fig. 6C), spleen (Fig. 6D), and liver (Fig. 6E) of infected mice. Histology analysis of cecal sections from these mice also indicated sever pathology with strong histopathological changes in mice that were infected with *S.* Typhimurium, but only light pathology with very mild histopathological changes in mice that were infected with *S.* Tirat-Zvi (Fig. 6F–K).

To characterize the level of inflammation induced by these pathogens in the mouse, RNA was extracted from the cecum and quantitative reverse transcription real-time PCR (qRT-PCR) was used to determine the expression of the proinflammatory cytokines IFNγ, IL-1β, IL-6, and TNF-α. As shown in Fig. S5, mice that were infected with *S.* Typhimurium elicited higher levels of inflammatory cytokines than mice infected with *S.* Tirat-Zvi (Fig. S5).

Collectively, these results indicated that while *S.* Tirat-Zvi is capable of colonizing young chicks at comparable levels as *S.* Typhimurium and causes inflammatory enterocolitis in this host, *S.* Tirat-Zvi can only moderately colonize the mouse host and does not elicit a severe inflammation as *S.* Typhimurium.

3. Discussion

The single species *S. enterica* is a vastly diverse bacterial species, containing as for 2014, 2637 antigenically distinct serovars [5]. Here, we reported the isolation and characterization of a yet unknown serovar, belonging to the super-lineage of *S.* Havana (HC2000_6515) that was isolated from a wild sparrow and presented a new monophasic antigenic formula of 13,23:i:-. Since *S. enterica* serovars are typically named after the geographical location where they were first isolated, we termed this new serovar *S. enterica* serovar Tirat-Zvi.

S. enterica serovars may be diverse in their pathogenicity, ecology and in their ability to infect, colonize and cause a disease in different hosts, a trait that is commonly referred as “host-specificity” [38]. While some serovars are host-specific and cause a disseminated septicemic disease in particular host species, other serovars are generalist with a wide host-specificity that allows

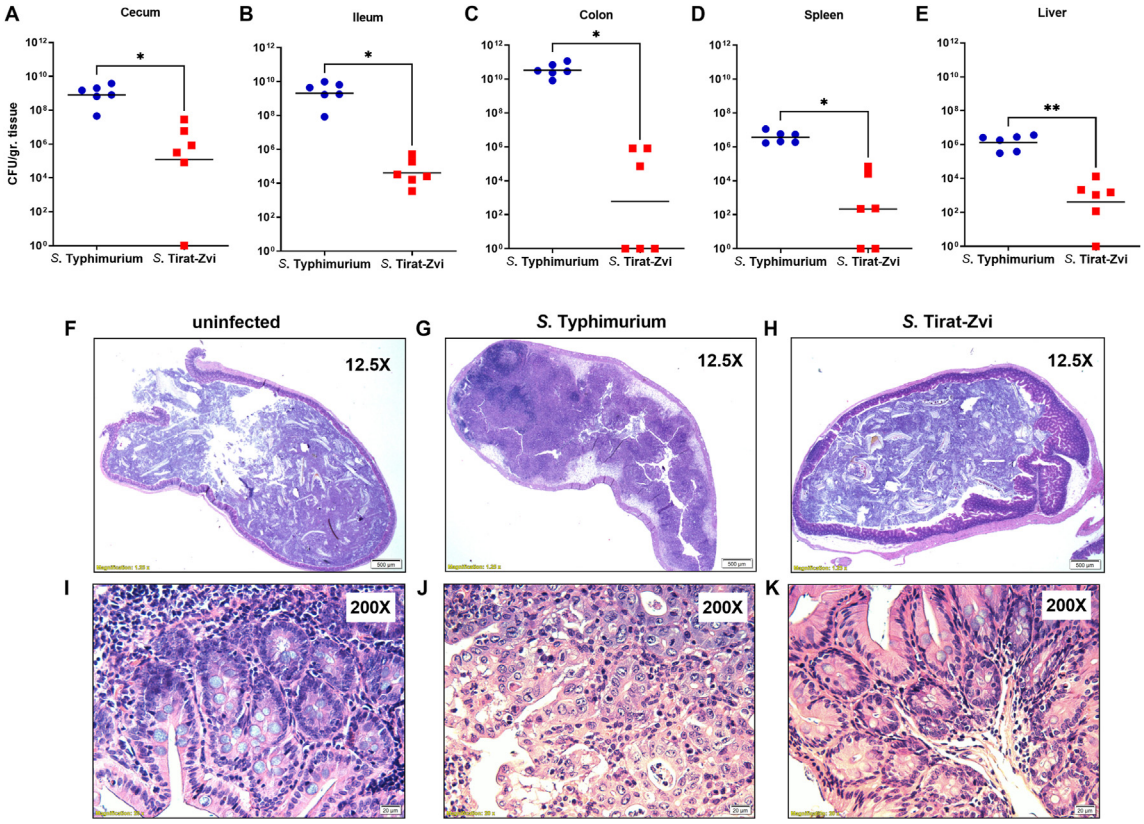

Fig. 6. *S.* Tirat-Zvi has impaired virulence in the mouse host. (**A**–**E**) Streptomycin pre-treated C57/BL6 mice were orally infected with 1×10^6 CFU of ampicillin resistance strains of *S.* Typhimurium SL1344 or *S.* Tirat-Zvi TZ282. Four days p.i., intestinal and systemic organs were harvested and homogenized. Serial dilutions of the homogenates were plated on selective XLD agar plates and bacterial loads per gram of tissue in the cecum (**A**), ileum (**B**), colon (**C**), spleen (**D**) and liver (**E**) were examined. Each dot represents the count from a single mouse and the geometric mean is indicated by the horizontal line. The gross appearance of paraffin embedded cecal sections is shown by ×12.5 magnification of H&E staining of cecal sections from an uninfected control (**F**) and mice infected with *S.* Typhimurium (**G**) or *S.* Tirat-Zvi (**H**). Bar = 500 μm. (**I**–**K**) ×200 magnifications of H&E staining are shown, bar = 20 μm.

them to promiscuously colonize and cause asymptomatic infection or gastroenteritis in a broad array of hosts [3,6]. Nevertheless, it is now becoming apparent that *Salmonella* classification at the serovar level does not provide the required resolution to capture host-specificity differences. For example, different pathovars of *S.* Typhimurium present distinct host-adaptation profiles including definitive phage type (DT) 40 and 56 to passerine birds, DT8 to ducks and geese, DT2 and DT99 to pigeons, U288 to swine and ST313 that causes an invasive salmonellosis in humans in sub Saharan Africa (reviewed in Ref. [6]). Recently, we reported the isolation and phenotypic characterization of a passerine-adapted monophasic *S.* Typhimurium strain in Israel and showed a significant genome degradation in multiple metabolic and virulence loci that were missing or inactivated compared to generalist *S.* Typhimurium pathovars [18].

Our understanding about the mechanisms underlying host-specificity is still limited. Recent comparative and functional genomics studies have shown that genomic decay resulted from gene deletion or gene inactivation (pseudogene formation) on one hand, and gene gain by horizontal acquisition on the other hand are common themes among host-adapted stains [6,39,40]. While, 123 out of 4575 annotated genes in *S.* Tirat-Zvi were predicted to be pseudogenes (Table S4), and no plasmid was identified in its genome, we did not find significant number of pseudogenes that are shared between S. Tirat-Zvi and the poultry-specific serovars *S.* Gallinarum or *S.* Pullorum [40]. Nevertheless, based on (i) its source of isolation, (ii) the fact that this serovar was never isolated from a clinical (human) sample (in Israel, *Salmonella* is a reportable pathogen and every clinical *Salmonella* isolate is serotyped and recorded), (iii) the presence of multiple pseudogenes and lack of plasmids and (iv) the pathological outcome in the different animal models, we hypothesize that *S.* Tirat-Zvi TZ282 may represent an evolutionary process of narrowing down its host-specificity to become an avian-adapted serovar. Yet, since this serovar was isolated once from one wild sparrow, definite classification of its host-specificity is difficult and further epidemiological evidences and additional experiments in other hosts are required to support this possibility.

The ability of a pathogen to infect a host is largely dependent on its capability to adhere to specific tissues, cells or receptors from that particular species. *Salmonella* utilizes a wide array of fimbrial organelles, surface-associated adhesins and flagella to actively make contact and adhere to host cells and facilitate colonization. As such, the precise combination of these factors and allelic variation in their sequence is thought to contribute to host-specificity and pathogenicity [41]. The largest group of known colonization factors is encoded by fimbrial operons of the chaperone-usher assembly class [42]. We found that *S.* Tirat-Zvi TZ282 genome encodes 14 chaperon-usher fimbria clusters, including the Fim (type 1 fimbria), Tcf, long polar fimbria (Lpf), and Ste fimbriae, which were previously proposed to play a role in the host-specificity of particular *S. enterica* pathovars [43–47].

One of the unique horizontally acquired regions identified in *S.* Tirat-Zvi was SPI-19, which is known to be present in several host-specific and host-adapted serovars, including *S.* Gallinarum, *S.* Pullorum and *S.* Dublin [29,30,48]. The role of the T6SS encoded

within SPI-19 in *Salmonella* pathogenicity is controversial and previous studies have reported conflicting conclusions. SPI-19 deletion in *S*. Pullorum resulted in a sharp decreased in invasion into and replication within chicken epithelial cells and macrophages as well as impaired colonization in chickens, during early time point [29]. Similarly, a SPI-19/T6SS deleted strain of *S*. Dublin presented impaired virulence in mice after oral infection. In contrast, SPI-19/T6SS was found to play no role during oral or intraperitoneal infection of chickens with *S*. Gallinarum [48]. In agreement with the latter, in *S*. Tirat-Zvi TZ282, SPI-19/T6SS was also found be dispensable for host cell invasion and replication and for colonization in young chicks (see Supplementary Material). Additionally, SPI-19/T6SS was not found to be required to compete with other bacteria during growth in rich and minimal medium in-vitro (data not shown). Nonetheless, we cannot exclude the possibility that SPI-19/T6SS may play a role in *S*. Tirat-Zvi virulence in different untested hosts or in older birds, with more complex microbiota communities.

Earlier analysis of metabolic models for 410 *Salmonella* strains from 64 different serovars have indicated growth differences that presumably reflect adaptation to particular hosts and colonization sites [49]. Interestingly, metabolic models (Table S5) and phenotypic microarray comparison between *S*. Tirat-Zvi and *S*. Typhimurium has indicated better utilization of multiple carbon sources by *S*. Tirat-Zvi than *S*. Typhimurium. We hypothesized that these differences are related to the distinct ecology of the serovars and possibly indicate colonization in animals with a vegetarian dietary pattern that is enriched in galactose, maltose and mannitol that is abundant in fruits, vegetables, seeds and grains.

S. Tirat-Zvi TZ282 genome was found to harbor the *ars* operon that mediates inorganic arsenic detoxification. A recent study has suggested that the presence of these genes in food-borne pathogens may be selected due to the use of arsenic compounds in insecticides, herbicides, and coccidiostats (antiprotozoal agents) in the agricultural sector and during food-producing animals farming and that arsenic tolerance is an adaptive phenotype for the ecological success of these strains [50]. Moreover, the ability of *S*. Tirat-Zvi TZ282 to readily form biofilm and the presence of the curli operon, further suggest that this strain has an environmental phase and that it can persist outside of its avian host.

In summary, we report the isolation of a new *S. enterica* serovar, designated *S*. Tirat-Zvi, from a wild sparrow in Israel. This new serovar is capable of causing an inflammatory enterocolitis in a young chick model, but is impaired in mice colonization and eliciting an inflammatory infection in the murine host compared to *S*. Typhimurium. Despite some evidence of genome degradation, this serovar is motile, can form high levels of biofilm on abiotic surfaces, efficiently utilizes maltose and various other carbon sources and is highly resistance to arsenic compounds. On the other hand, this serovar presented inferior invasion into non phagocytic host cells compared to *S*. Typhimurium. We hypothesize that this collection of phenotypic differences reflects the unique ecological niche of this serovar and its evolutionary adaptation to wild birds, as a permissive host. Moreover, identification of a new *S. enterica* serovar with a distinct phenotypic portfolio demonstrates the vast genetic and phenotypic diversity of this continuously evolving pathogen and its complex interaction with the environment and hosts.

Declaration of competing interest

The authors declare no competing interests.

Acknowledgments

This work was supported by grant numbers: I-41-416.6-2017 from the German-Israeli Foundation for Scientific Research and Development (GIF; http://www.gif.org.il/Pages/default.aspx); A128055 from the VolkswagenStiftung Research Cooperation Lower Saxony—Israel (https://www.volkswagenstiftung.de/en/funding/our-funding-portfolio-at-a-glance/nieders%C3%A4chsisches-vorab-research-cooperation-lower-saxony-%E2%80%93-israel), and grant number 2616/18 from the joint ISF-Broad Institute program (https://www.isf.org.il/) awarded to OGM. The funders had no role in study design, data collection and interpretation, or the decision to submit the work for publication. We are thankful to Dr. Maya Davidovich-Cohen and the National *Salmonella* Reference Center for their help in serotyping the sparrow isolates, for Dr. Omri Bauer from Biovac Ltd. for valuable help in the chick model and to Dr. Asaf Berkowitz from the Department of Avian Diseases at the Kimron Veterinary Institute for his input in histology and pathology analysis. We are grateful to Prof. Dr. Guntram Grassl from the Hannover Medical School for helpful discussions and critical reading of the manuscript.

Appendix A. Supplementary data

Supplementary data to this article can be found online at https://doi.org/10.1016/j.micinf.2023.105249.

References

[1] Uzzau S, Brown DJ, Wallis T, Rubino S, Leori G, Bernard S, et al. Host adapted serotypes of *Salmonella enterica*. Epidemiol Infect 2000;125:229–55.
[2] Schikora A, Garcia AV, Hirt H. Plants as alternative hosts for Salmonella. Trends Plant Sci 2012;17:245–9.
[3] Gal-Mor O. Persistent infection and long-term carriage of typhoidal and nontyphoidal salmonellae. Clin Microbiol Rev 2019;32.
[4] Majowicz SE, Musto J, Scallan E, Angulo FJ, Kirk M, O'Brien SJ, et al. The global burden of nontyphoidal Salmonella gastroenteritis. Clin Infect Dis 2010;50:882–9.
[5] Issenhuth-Jeanjean S, Roggentin P, Mikoleit M, Guibourdenche M, de Pinna E, Nair S, et al. Supplement 2008-2010 (no. 48) to the White-Kauffmann-Le Minor scheme. Res Microbiol 2014;165:526–30.
[6] Stevens MP, Kingsley RA. Salmonella pathogenesis and host-adaptation in farmed animals. Curr Opin Microbiol 2021;63:52–8.
[7] Wallis TS, Barrow PA. Salmonella epidemiology and pathogenesis in food-producing animals. EcoSal Plus 2005;1.
[8] Barrow PA, Freitas Neto OC. Pullorum disease and fowl typhoid–new thoughts on old diseases: a review. Avian Pathol 2011;40:1–13.
[9] Kingsley RA, Baumler AJ. Host adaptation and the emergence of infectious disease: the *Salmonella* paradigm. Mol Microbiol 2000;36:1006–14.
[10] Humphries AD, Townsend SM, Kingsley RA, Nicholson TL, Tsolis RM, Baumler AJ. Role of fimbriae as antigens and intestinal colonization factors of Salmonella serovars. FEMS Microbiol Lett 2001;201:121–5.
[11] Stevens MP, Humphrey TJ, Maskell DJ. Molecular insights into farm animal and zoonotic Salmonella infections. Philos Trans R Soc Lond B Biol Sci 2009;364:2709–23.
[12] Johnson R, Mylona E, Frankel G. Typhoidal Salmonella: distinctive virulence factors and pathogenesis. Cell Microbiol 2018;20:e12939.
[13] Abrahams GL, Hensel M. Manipulating cellular transport and immune responses: dynamic interactions between intracellular Salmonella enterica and its host cells. Cell Microbiol 2006;8:728–37.
[14] Bawn M, Alikhan NF, Thilliez G, Kirkwood M, Wheeler NE, Petrovska L, et al. Evolution of Salmonella enterica serotype Typhimurium driven by anthropogenic selection and niche adaptation. PLoS Genet 2020;16:e1008850.
[15] Kingsley RA, Kay S, Connor T, Barquist L, Sait L, Holt KE, et al. Genome and transcriptome adaptation accompanying emergence of the definitive type 2 host-restricted Salmonella enterica serovar Typhimurium pathovar. mBio 2013;4. e00565-13.
[16] Hughes LA, Shopland S, Wigley P, Bradon H, Leatherbarrow AH, Williams NJ, et al. Characterisation of Salmonella enterica serotype Typhimurium isolates from wild birds in northern England from 2005 - 2006. BMC Vet Res 2008;4:4.
[17] Mather AE, Lawson B, de Pinna E, Wigley P, Parkhill J, Thomson NR, et al. Genomic analysis of Salmonella enterica serovar Typhimurium from wild passerines in England and Wales. Appl Environ Microbiol 2016;82:6728–35.

[18] Cohen E, Azriel S, Auster O, Gal A, Zitronblat C, Mikhlin S, et al. Pathoadaptation of the passerine-associated Salmonella enterica serovar Typhimurium lineage to the avian host. PLoS Pathog 2021;17:e1009451.
[19] Li W, O'Neill KR, Haft DH, DiCuccio M, Chetvernin V, Badretdin A, et al. RefSeq: expanding the Prokaryotic Genome Annotation Pipeline reach with protein family model curation. Nucleic Acids Res 2021;49:D1020–8.
[20] Achtman M, Zhou Z, Charlesworth J, Baxter L. EnteroBase: hierarchical clustering of 100 000s of bacterial genomes into species/subspecies and populations. Philos Trans R Soc Lond B Biol Sci 2022;377:20210240.
[21] Zhou Z, Alikhan NF, Sergeant MJ, Luhmann N, Vaz C, Francisco AP, et al. GrapeTree: visualization of core genomic relationships among 100,000 bacterial pathogens. Genome Res 2018;28:1395–404.
[22] Datsenko KA, Wanner BL. One-step inactivation of chromosomal genes in Escherichia coli K-12 using PCR products. Proc Natl Acad Sci U S A 2000;97:6640–5.
[23] Gibson DG, Young L, Chuang RY, Venter JC, Hutchison 3rd CA, Smith HO. Enzymatic assembly of DNA molecules up to several hundred kilobases. Nat Methods 2009;6:343–5.
[24] Elhadad D, Desai P, Grassl GA, McClelland M, Rahav G, Gal-Mor O. Differences in host cell invasion and SPI-1 expression between Salmonella enterica serovar Paratyphi A and the non-typhoidal serovar Typhimurium. Infect Immun 2016;84:1150–65.
[25] Azriel S, Goren A, Rahav G, Gal-Mor O. The stringent response regulator DksA is required for Salmonella enterica serovar Typhimurium growth in minimal medium, motility, biofilm formation, and intestinal colonization. Infect Immun 2016;84:375–84.
[26] Alikhan NF, Zhou Z, Sergeant MJ, Achtman M. A genomic overview of the population structure of Salmonella. PLoS Genet 2018;14:e1007261.
[27] Achtman M, Zhou Z, Alikhan NF, Tyne W, Parkhill J, Cormican M, et al. Genomic diversity of Salmonella enterica -the UoWUCC 10K genomes project. Wellcome Open Res 2020;5:223.
[28] Achtman M, Wain J, Weill FX, Nair S, Zhou Z, Sangal V, et al. Multilocus sequence typing as a replacement for serotyping in Salmonella enterica. PLoS Pathog 2012;8:e1002776.
[29] Xian H, Yuan Y, Yin C, Wang Z, Ji R, Chu C, et al. The SPI-19 encoded T6SS is required for Salmonella Pullorum survival within avian macrophages and initial colonization in chicken dependent on inhibition of host immune response. Vet Microbiol 2020;250:108867.
[30] Blondel CJ, Yang HJ, Castro B, Chiang S, Toro CS, Zaldivar M, et al. Contribution of the type VI secretion system encoded in SPI-19 to chicken colonization by Salmonella enterica serotypes Gallinarum and Enteritidis. PLoS One 2010;5:e11724.
[31] Amaya FA, Blondel CJ, Barros-Infante MF, Rivera D, Moreno-Switt AI, Santiviago CA, et al. Identification of type VI secretion systems effector proteins that contribute to interbacterial competition in Salmonella Dublin. Front Microbiol 2022;13:811932.
[32] Gal-Mor O, Finlay BB. Pathogenicity islands: a molecular toolbox for bacterial virulence. Cell Microbiol 2006;8:1707–19.
[33] Aziz RK, Bartels D, Best AA, DeJongh M, Disz T, Edwards RA, et al. The RAST Server: rapid annotations using subsystems technology. BMC Genomics 2008;9:75.
[34] Li J, Smith NH, Nelson K, Crichton PB, Old DC, Whittam TS, et al. Evolutionary origin and radiation of the avian-adapted non-motile salmonellae. J Med Microbiol 1993;38:129–39.
[35] Kang X, Zhou X, Tang Y, Jiang Z, Chen J, Mohsin M, et al. Characterization of two-component system CitB family in Salmonella Pullorum. Int J Mol Sci 2022;23.
[36] Elhadad D, Desai P, Rahav G, McClelland M, Gal-Mor O. Flagellin is required for host cell invasion and normal Salmonella pathogenicity island 1 expression by Salmonella enterica serovar Paratyphi A. Infect Immun 2015;83:3355–68.
[37] Aviv G, Cornelius A, Davidovich M, Cohen H, Suwandi A, Galeev A, et al. Differences in the expression of SPI-1 genes pathogenicity and epidemiology between the emerging Salmonella enterica serovar Infantis and the model Salmonella enterica serovar Typhimurium. J Infect Dis 2019;220:1071–81.
[38] Baumler A, Fang FC. Host specificity of bacterial pathogens. Cold Spring Harb Perspect Med 2013;3.
[39] Hiyoshi H, Wangdi T, Lock G, Saechao C, Raffatellu M, Cobb BA, et al. Mechanisms to evade the phagocyte respiratory burst arose by convergent evolution in typhoidal Salmonella serovars. Cell Rep 2018;22:1787–97.
[40] Langridge GC, Fookes M, Connor TR, Feltwell T, Feasey N, Parsons BN, et al. Patterns of genome evolution that have accompanied host adaptation in Salmonella. Proc Natl Acad Sci U S A 2015;112:863–8.
[41] Yue M, Schifferli DM. Allelic variation in Salmonella: an underappreciated driver of adaptation and virulence. Front Microbiol 2014;4:419.
[42] Nuccio SP, Baumler AJ. Evolution of the chaperone/usher assembly pathway: fimbrial classification goes Greek. Microbiol Mol Biol Rev 2007;71:551–75.
[43] Azriel S, Goren A, Shomer I, Aviv G, Rahav G, Gal-Mor O. The Typhi colonization factor (Tcf) is encoded by multiple non-typhoidal Salmonella serovars but exhibits a varying expression profile and interchanging contribution to intestinal colonization. Virulence 2017;8:1791–807.
[44] De Masi L, Yue M, Hu C, Rakov AV, Rankin SC, Schifferli DM. Cooperation of adhesin alleles in Salmonella-host tropism. mSphere 2017;2.
[45] Dufresne K, Saulnier-Bellemare J, Daigle F. Functional analysis of the chaperone-usher fimbrial gene clusters of Salmonella enterica serovar Typhi. Front Cell Infect Microbiol 2018;8:26.
[46] Kisiela DI, Chattopadhyay S, Libby SJ, Karlinsey JE, Fang FC, Tchesnokova V, et al. Evolution of Salmonella enterica virulence via point mutations in the fimbrial adhesin. PLoS Pathog 2012;8:e1002733.
[47] Townsend SM, Kramer NE, Edwards R, Baker S, Hamlin N, Simmonds M, et al. *Salmonella enterica* serovar Typhi possesses a unique repertoire of fimbrial gene sequences. Infect Immun 2001;69:2894–901.
[48] Schroll C, Huang K, Ahmed S, Kristensen BM, Pors SE, Jelsbak L, et al. The SPI-19 encoded type-six secretion-systems (T6SS) of Salmonella enterica serovars Gallinarum and Dublin play different roles during infection. Vet Microbiol 2019;230:23–31.
[49] Seif Y, Kavvas E, Lachance JC, Yurkovich JT, Nuccio SP, Fang X, et al. Genome-scale metabolic reconstructions of multiple Salmonella strains reveal serovar-specific metabolic traits. Nat Commun 2018;9:3771.
[50] Mourao J, Rebelo A, Ribeiro S, Peixe L, Novais C, Antunes P. Tolerance to arsenic contaminant among multidrug-resistant and copper-tolerant Salmonella successful clones is associated with diverse ars operons and genetic contexts. Environ Microbiol 2020;22:2829–42.